



## Simple and facile approach to synthesize magnetite nanoparticles and assessment of their effects on blood cells

Luiz F. Cótica<sup>a,\*</sup>, Valdirlei F. Freitas<sup>a</sup>, Gustavo S. Dias<sup>a</sup>, Ivair A. Santos<sup>a</sup>, Sheila C. Vendrame<sup>b</sup>, Najeh M. Khalil<sup>b</sup>, Rubiana M. Mainardes<sup>b</sup>, Margo Staruch<sup>c</sup>, Menka Jain<sup>c</sup>

<sup>a</sup> Department of Physics, Universidade Estadual de Maringá, Maringá, PR 87020900, Brazil

<sup>b</sup> Department of Pharmacy, Universidade Estadual do Centro-Oeste, Guarapuava, PR 85040080, Brazil

<sup>c</sup> Department of Physics, University of Connecticut, Storrs, CT 06269, USA

### ARTICLE INFO

#### Article history:

Received 13 May 2011

Received in revised form

17 August 2011

Available online 1 September 2011

#### Keywords:

Magnetite nanoparticle

Structural property

Magnetic property

Biological effect

### ABSTRACT

In this paper, a very simple and facile approach for the large scale synthesis of uniform and size-controllable single-domain magnetite nanoparticles is reported. These magnetite nanoparticles were synthesized via thermal decomposition of a ferric nitrate/ethylene glycol solution. The structural and morphological properties of the synthesized nanoparticles were carefully studied. Nearly spherical nanoparticles with inverted spinel structure and average particle and crystallite sizes smaller than 20 nm were obtained. The magnetic measurements revealed that magnetite nanoparticles have a magnetic saturation value near that of the bulk magnetite. The erythrocyte cytotoxicity assays showed no hemolytic potential of the samples containing magnetite nanoparticles, indicating no cytotoxic activity on human erythrocytes, which makes these interesting for biotechnological applications.

© 2011 Elsevier B.V. All rights reserved.

### 1. Introduction

In the recent years, many researchers have investigated materials designed to accomplish multiple performance objectives using a single system [1,2], i.e., materials with multiple functionalities for their applications in electronics, energy, and medicine [3–6]. With the advancement in nanotechnology it has become possible to fabricate, characterize, and specially tailor the multifunctional properties of nanoparticles. For example, in biomedical applications, water or alcohol dispersible magnetic nanoparticles allowed new opportunities as contrast agents for magnetic resonance imaging [7], magnetic field guided drug delivery [8], tumor treatment via hyperthermia [9] and biomolecular separation, and diagnostic imaging [10,11]. Especially in drug delivery applications, drug transport through magnetic nanoparticles has been widely studied in an attempt to obtain particles with high drug carrier capacity, good stability in aqueous solutions, and good biocompatibility with cells and tissues [12].

A variety of magnetic nanoparticles composed of different atoms or ions with different magnetic moments have been synthesized to target these applications. Inorganic nanoparticles such as Fe<sub>3</sub>O<sub>4</sub> (magnetite),  $\gamma$ -Fe<sub>2</sub>O<sub>3</sub> (maghemite), and spinel-structured magnetic nanoparticles (MFe<sub>2</sub>O<sub>4</sub>, M=Fe, Co, Ni, and

Mn) have been widely used for their applications in nanomedicine [13]. Among various magnetic nanoparticles, magnetite offers many attractive possibilities in biomedicine and thus is of great importance [12]. Bulk and nanostructured magnetites crystallize with inverted spinel structure (space group *Fd3m*) and the large oxygen ions are closely packed in a cubic arrangement, while smaller Fe-ions fill the structural gaps (tetrahedral and octahedral sites). The tetrahedral and octahedral sites form two magnetic sublattices, A and B, respectively. This particular arrangement of cations in A and B sublattices characterizes the inverse spinel structure. With negative AB exchange interactions, the net magnetic moment of the magnetite is due to the B-site Fe<sup>2+</sup> ions [14].

The magnetite nanoparticles have a controllable size ranging from a few nanometers up to tens of nanometers, which is comparable to the dimensions of some cells (10–100  $\mu$ m), viruses (20–450 nm), proteins (5–50 nm), or genes (2 nm wide and 10–100 nm long). This means that these nanoparticles are of great interest for their use with the biological entities of interest since they are biocompatible and able to interact or bind to target cells [13,15,16]. To date, several methods have been proposed to synthesize magnetite nanoparticles [17–24]. In general, these methods are wet chemical routes. The most widely used method is based on the co-precipitation of Fe<sup>2+</sup> and Fe<sup>3+</sup> aqueous salt solutions by addition of a base [17]. The size, shape, and composition of synthesized nanoparticles depend on the type of salts used (chlorides, sulphates, nitrates, etc.), Fe<sup>2+</sup>/Fe<sup>3+</sup> ratio,

\* Corresponding author. Tel.: +55 44 3011 5904; fax: +55 44 3263 4623.  
E-mail address: [lfcotica@pq.cnpq.br](mailto:lfcotica@pq.cnpq.br) (L.F. Cótica).

and the pH and ionic strength of the media [18,19], but the disadvantage of this method is that the synthesis of particles must be done in an oxygen-free environment [20]. Other methods based on the precipitation principle have been developed: sol-gel [21], polymer matrix-mediated synthesis [5], and precipitation using microemulsions [22,23] and vesicles [24]. In all these routes, just small quantities of nanoparticles can be produced.

Herein, we report a very simple and facile approach for the large scale synthesis of uniform and size-controllable single-domain magnetite nanoparticles with diameters smaller than 20 nm. Structural, microstructural, and magnetic properties of these nanoparticles are presented and discussed. Attestation of potential for biological applications was obtained by erythrocyte cytotoxicity assays that showed no hemolytic potential and negligible toxicity for samples containing magnetite nanoparticles processed by the innovative route proposed in this work.

## 2. Experimental

### 2.1. Preparation of magnetite nanoparticles

The magnetite nanoparticles were synthesized via thermal decomposition of a ferric nitrate/ethylene glycol solution—see Fig. 1(a). First, a mixture of adequate amounts of ferric nitrate (Alfa Aesar) and ethylene glycol (Vetec) was prepared. The solution was homogenized for 1 h, at room temperature followed by heating at 90 °C (Fig. 1(b)). To obtain nanoparticles with different sizes and distributions, the resulting material was heated in a tube furnace at temperatures between 300 °C (sample MAG300) and 500 °C (sample MAG500), under inert atmosphere (argon)—Fig. 1(c) and (d). Results from other samples were not included because they are similar to those of the above mentioned samples.

### 2.2. Characterization of nanoparticles

X-ray diffraction (XRD) measurements were performed with a Shimadzu XRD 7000 diffractometer, using  $\text{CuK}_\alpha$  radiation. The mean crystallite sizes were calculated from the linewidth broadening relative to a  $\text{LaB}_6$  standard using Scherrer's formula [25]. Morphological characterizations were conducted in a JEOL JEM-1400 Transmission Electron Microscope (TEM) in order to gain some insights of the microstructure and the particle sizes distribution. Temperature dependent and field dependent magnetic characterizations (at 300 K) were performed in a commercial Vibrating Sample Magnetometer (VSM) from Lakeshore and in a VSM attached with a Physical Property Measurement System from Quantum Design.

### 2.3. Preparation of erythrocyte suspensions

The in vitro cytotoxic effects of magnetite nanoparticles were studied using heparinized venous blood samples collected from healthy volunteers. Whole blood was centrifuged (4000 rpm for

5 min) at 4 °C using a refrigerated centrifuge and the plasma and buffy coat were removed by aspiration. The red blood cells were washed three times by centrifugation (4000 rpm for 5 min) in cold phosphate buffer saline (PBS; 0.15 mM NaCl, 10 mM sodium phosphate, pH 7.4). The supernatant and buffy coat of white cells was carefully removed with each wash. The red blood cells were finally resuspended with the same buffer to obtain a hematocrit of 1% [26]. This suspension was used for erythrocyte hemolysis and measurement of  $\text{K}^+$  assays. All experiments involving human blood were approved by the Ethics Committee of the Universidade Estadual do Centro-Oeste (protocol 313/2010).

### 2.4. Erythrocyte hemolysis assay

Different concentrations of MAG300 and MAG500 nanoparticles were incubated with a 1% red blood cell suspension for 24 h at 37 °C with constant shaking, in PBS with 30 mg/mL penicillin and 50 mg/mL streptomycin solution. After incubation, the red blood cell suspension was centrifuged at 4000 rpm for 5 min. Hemolysis was determined by measuring the absorbance at 540 nm in a microplate reader (UV-vis spectrometer Molecular Devices SpectraMax 190) [27,28].

### 2.5. $\text{K}^+$ release

Red blood cells were incubated with different concentrations of MAG300 and MAG500 nanoparticles for 24 h at 37 °C with constant shaking. After the incubation, the red blood cells were centrifuged at 4000 rpm at 4 °C for 5 min, and  $\text{K}^+$  release was measured with an ion-selective electrode (Roche/AVL 9180).

## 3. Results and discussion

### 3.1. Physical properties—structural, microstructural, and magnetic properties

The XRD results ( $\theta$ – $2\theta$  scans) for MAG300 and MAG500 samples (Fig. 2) showed broadened lines, which were assigned to the crystallized magnetite (JCPDS PDF19-0629) with inverted spinel structure (space group  $Fd\bar{3}m$ ) [14]. The mean crystallite sizes ( $t$ ) obtained using Scherrer's formula [25] ( $t = 0.9\lambda/B \cos \theta$ , where  $B$  is the half-value breadth of the diffracted X-ray beam,  $\theta$  is the Bragg angle, and  $\lambda$  is the wavelength of the incident X-rays) were  $t_{\text{MAG300}} = 15$  nm and  $t_{\text{MAG500}} = 20$  nm for 300 °C and 500 °C annealed samples, respectively.

TEM images for MAG300 and MAG500 nanoparticles are shown in Fig. 3(a) and (b), respectively. In both samples, the majority of the particles were nearly spherical in shape. Some magnetite nanoparticles are partially superimposed onto the agglomerate core, i.e., the boundary limit of each nanoparticle is partially diffuse; thus a precise average particle size cannot be determined. However, a narrowed particle sizes distribution can be seen and the average particle size for the magnetite nanoparticles was found to be between 15 and 20 nm. It should be noted

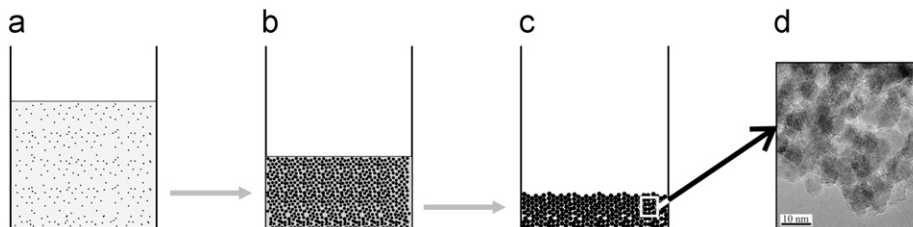
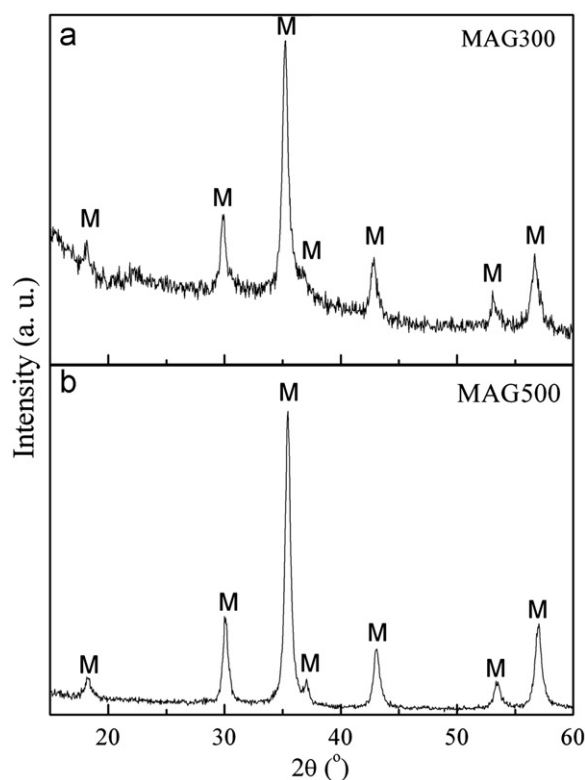


Fig. 1. A schematic of the flowchart for the synthesis of magnetite nanoparticles.



**Fig. 2.** X-ray diffraction patterns for the magnetite nanoparticles synthesized at (a) 300 °C (MAG300) and (b) 500 °C (MAG500). M=magnetite (JCPDS PDF19-0629).

that generally, magnetite nanoparticles with no surface treatments tend to agglomerate with the neighboring ones, which could be due to the substantial built-up specific surface area of the nanosized particles [29]. Also, the magnetic nanoparticles aggregated together to reduce their surface energy [30] and/or due to the magnetic dipole–dipole interactions and the van der Waals forces between the nanoparticles [31,32].

Fig. 4 plots the magnetization vs. applied field ( $M$  vs.  $H$ ) curves for MAG300 and MAG500 samples and the value of saturation magnetization ( $M_s$ ) was found to be 11 emu/g for MAG300 and 67 emu/g for MAG500.  $M_s$  was found to increase with an increase in the annealing temperature and approached that of the bulk magnetite (92 emu/g) [12]. The increase of  $M_s$  can be explained by considering that the annealing contributes to facilitate the exchange interaction between the magnetic sublattices of the magnetic core ( $\text{Fe}_3\text{O}_4$ ) and to increase the magnetic core, reducing the surface spin effects [14]. In order to better define the magnetic state of the magnetite nanoparticles, field cooling (FC) and zero field cooling (ZFC) magnetization values were measured (as shown in Fig. 5). All measurements were performed with an applied DC field of 20 Oe. No thermoremanent behavior was observed in these curves of both samples, as previously reported [14]. In fact, nanosized magnetic particles are expected to be magnetic monodomain particles and the temperature dependence of the thermoremanent magnetization directly correlates with the deblocking process that occurs inside the magnetic nanoparticle system for temperature increases in zero applied magnetic fields and after a previous FC process. As previously reported [14,33], the blocking temperature ( $T_B$ ) that was obtained from the temperature dependent ZFC and FC curves was near room temperature. This behavior is expected since the magnetic properties of nanoparticles are strongly influenced by finite size effects and the breaking of the crystal symmetry at the particle

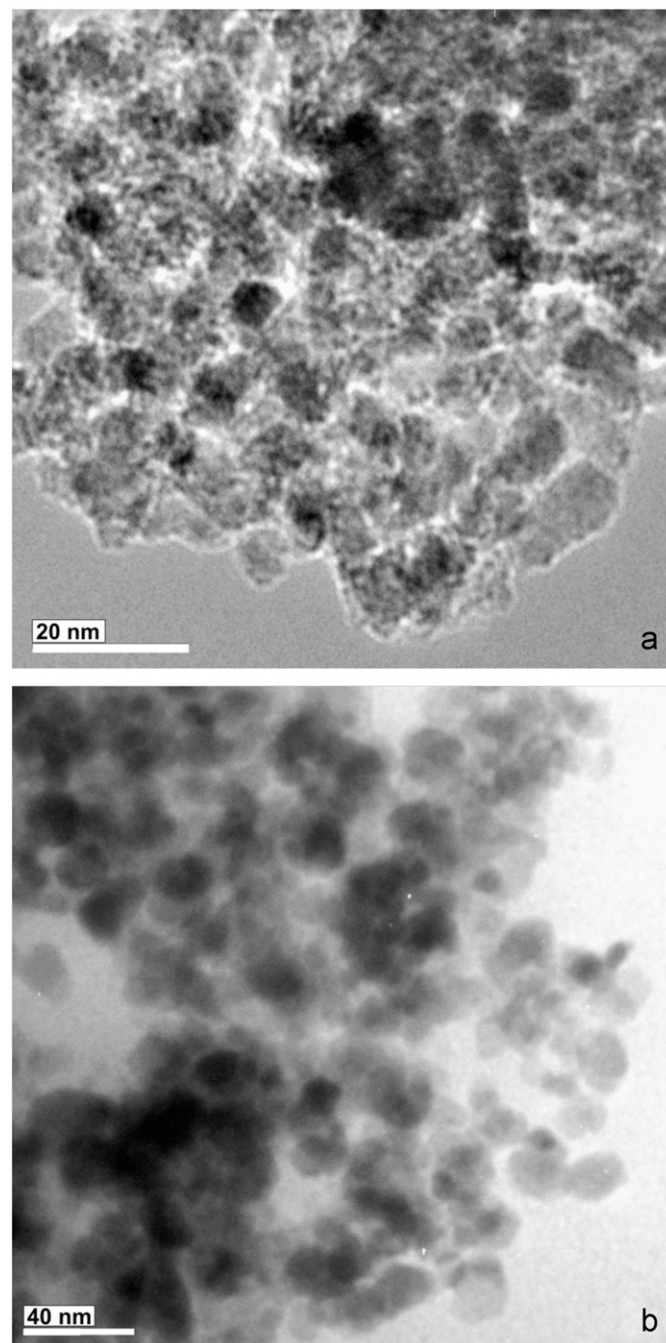


**Fig. 3.** Transmission electron microscopy images of magnetite nanoparticles synthesized at (a) 300 °C (MAG300) and (b) 500 °C (MAG500).

surface. In that case, very high anisotropy constant values suppress the thermoremanent behavior [14].

### 3.2. Cytotoxicity assays

Magnetite nanoparticles have been of significant use for many different technological areas, especially in biomedical applications. However, for use in biological systems they should have biocompatibility with cells and tissues among other properties. Several tests have been performed in order to evaluate the toxicological risks of magnetite nanoparticles [34], including the evaluation of cytotoxicity on red blood cells and phagocyte cells [35–38].

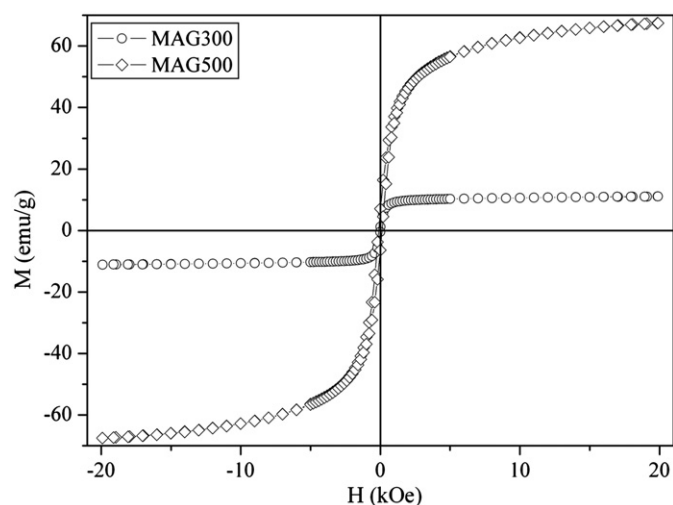


**Fig. 4.** Room temperature magnetization vs. magnetic field data (M vs. H) of magnetite nanoparticles synthesized at (a) 300 °C (MAG300) and (b) 500 °C (MAG500).

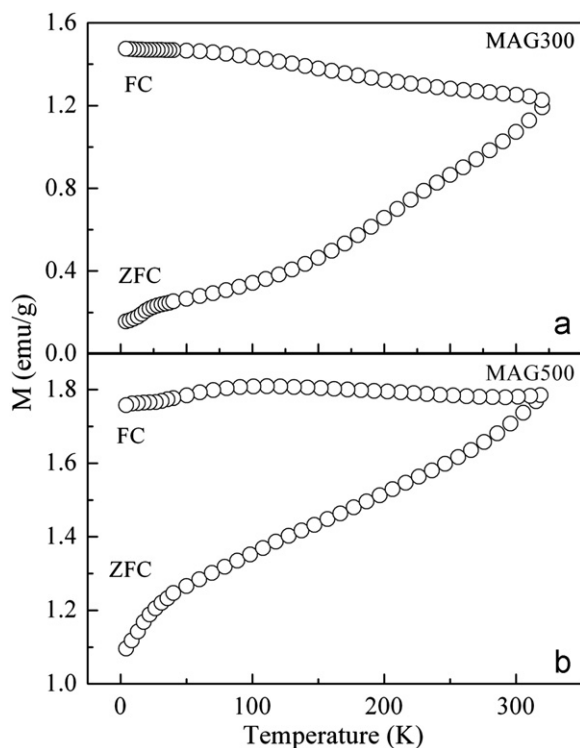


**Fig. 5.** Temperature dependent magnetization (field cooling and zero field cooling) of magnetite nanoparticles synthesized at (a) 300 °C (MAG300) and (b) 500 °C (MAG500).

Several studies also use erythrocytes as a model to assess cytotoxicity of a series of compounds that have some potential biological activity and that have not yet been evaluated for toxic effects by other methods. Hemolysis testing is a fast, efficient, simple, and low cost analysis method to evaluate the possible cytotoxicity of magnetite nanoparticles on erythrocytes membrane, determined spectrophotometrically by observing the release of hemoglobin. Fig. 6 shows representative results obtained by spectroscopic measurements. The incubation (suspension of cells in saline with some volume of magnetite nanoparticles) for 24 h with different concentrations of MAG300 and MAG500 (0.062–1.87 mg/mL) promoted a rate of hemolysis

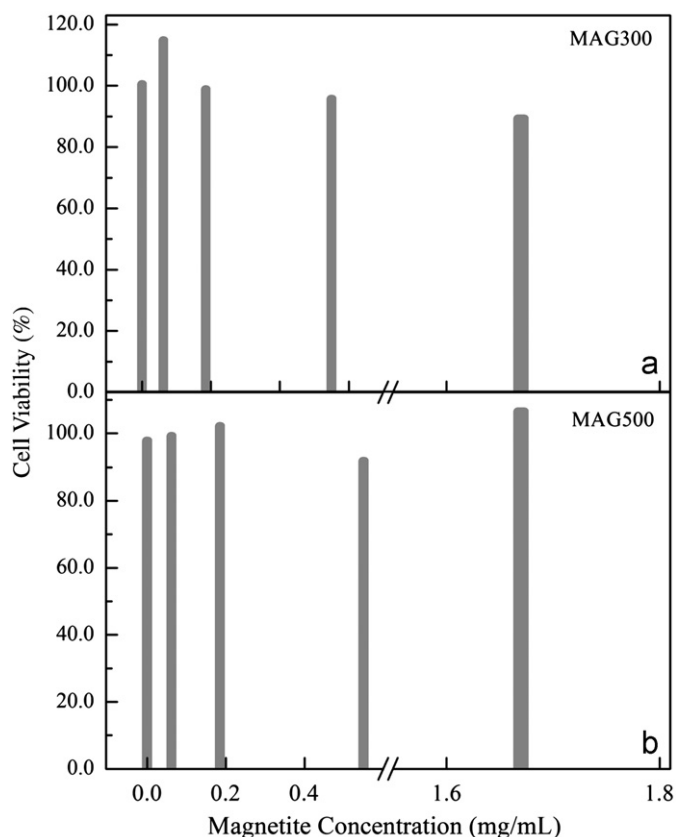


**Fig. 6.** Hemolysis test on human erythrocytes with increasing concentrations of magnetite nanoparticles synthesized at (a) 300 °C (MAG300) and (b) 500 °C (MAG500).

similar to that of control sample (suspension of cells in the absence of nanoparticles), i.e., MAG300 and MAG500 nanoparticles promoted no significant hemolysis in these blood cells. Corroborating with hemolysis results, the analysis of K-release of red blood cells, which is also an indicator of membrane damage, showed similar results (data not shown). Thus, the cytotoxicity assays indicate that MAG300 and MAG500 nanoparticles have no effects on blood cells that were potentially in contact with these particles in circulation, demonstrating their potentiality for nanomedicine and biotechnological applications.

#### 4. Conclusion

In this study, we report a very simple approach for the large scale synthesis of uniform and size-controllable single-domain magnetite nanoparticles. Based on X-ray diffraction and transmission electron microscopy, it was inferred that the magnetite nanoparticles were of spherical shape with diameters smaller than 20 nm and narrow size distribution. Magnetic saturation close to the bulk magnetite was confirmed with magnetic measurements. Assays using human erythrocytes were performed to evaluate the cytotoxicity of these magnetite nanoparticles. The erythrocyte cytotoxicity assays showed no hemolytic potential of the samples containing magnetites. Thus, we can conclude that the magnetite nanoparticles have no cytotoxic activity on human erythrocytes.

These results clearly indicate that the present magnetite nanoparticles can be a model drug-carrier, which makes these interesting for their potential use in other biomedical applications, such as DNA separation, drug delivery site-specific, cancer treatment by hyperthermia, and diagnostic imaging in MRI.

Further, this new route of nanoparticles synthesis would simplify and reduce the cost of production, providing access to drugs and carriers that utilize these nanoparticles to a large number of people.

## Acknowledgements

The authors would like to thank the CAPES (Proc. 082/2007), CNPq (Proc. 307102/2007-2 and 302748/2008-3), and Fundação Araucária de Apoio ao Desenvolvimento Científico e Tecnológico do Paraná (Prot. 15727) Brazilian agencies for their financial support. S.C.V. also thanks the Fundação Araucária for the fellowship. We also gratefully acknowledge the instrumental research facilities provided by COMCAP/UEM. Author M.J. is grateful for the support from the National Science Foundation Grant (NSF1105975).

## References

- [1] N.A. Spaldin, M. Fiebig, *Science* 309 (2005) 391.
- [2] J.F. Scott, *Science* 315 (2007) 954.
- [3] M. Fiebig, *Journal of Physics D: Applied Physics* 38 (2005) R123.
- [4] A. Balazs, C. Emrick, T.P. Russell, *Science* 314 (2006) 1107.
- [5] R.F. Ziolo, et al., *Science* 257 (1992) 219.
- [6] H. Kawaguchi, *Progress in Polymer Science* 25 (2000) 1171.
- [7] D.K. Kim, et al., *Chemical Materials* 15 (2003) 4343.
- [8] R. Asmatulu, et al., *Journal of Magnetism and Magnetic Materials* 292 (2005) 108.
- [9] J. Roger, et al., *The European Physical Journal—Applied Physics* 5 (1999) 321.
- [10] P.A. Liberti, C.G. Rao, L.W.M.M. Terstappen, *Journal of Magnetism and Magnetic Materials* 225 (2001) 301.
- [11] D. Navarathne, et al., *Material Letters* 65 (2011) 219.
- [12] R.B. Gupta, U.B. Kompella, *Nanoparticle Technology for Drug Delivery*, Taylor & Francis Group, New York, 2006.
- [13] J. Yang, et al., *International Journal of Pharmacy* 324 (2006) 185.
- [14] L.F. Cótica, et al., *Journal of Applied Physics* 108 (2010) 064325.
- [15] Q.A. Pankhurst, et al., *Journal of Physics D* 36 (2003) 167.
- [16] R.H. Muller, et al., *International Journal of Pharmacy* 138 (1996) 85.
- [17] G.W. Reimers, S.E. Khalafalla, US Bureau Mines Technical Report, 59, 1972.
- [18] G.C. Hadjipanayis, R.W. Siegel, *Nanophase Materials: Synthesis, Properties and Applications—NATO ASI Series*, Kluwer, Dordrecht, 1993.
- [19] C.E. Sjogren, et al., *Magnetic Resonance in Medicine* 31 (1994) 268.
- [20] A.K. Gupta, A.S.G. Curtis, *Biomaterials* 25 (2004) 3029.
- [21] T.M. Tillotson, et al., *Journal of Non-Crystalline Solids* 285 (2001) 335.
- [22] Y. Deng, et al., *Journal of Magnetism and Magnetic Materials* 257 (2003) 69.
- [23] S. Santra, et al., *Langmuir* 17 (2001) 2900.
- [24] S. Li, et al., *Colloids and Surfaces A* 174 (2000) 275.
- [25] A.L. Patterson, *Physical Review* 56 (1939) 978.
- [26] C.D. Hapner, P. Deuster, Y. Chen, *Chemistry–Biology Interaction* 186 (2010) 275.
- [27] A. Banerjee, et al., *Chemistry–Biology Interaction* 174 (2008) 134.
- [28] J. Wang, et al., *Food and Chemical Toxicology* 47 (2009) 1591.
- [29] D.H. Chen, X.R. He, *Materials Research Bulletin* 36 (2001) 1369.
- [30] C. Hu, Z. Gao, X. Yang, *Chemical Physics Letters* 429 (2006) 513.
- [31] Y. Lalatonne, J. Richardi, M.P. Pileni, *Nature Materials* 3 (2004) 121.
- [32] P.A. Hartley, G.D. Parfitt, L.B. Pollack, *Powder Technology* 42 (1985) 35.
- [33] R.A. Silva, et al., *Journal of Solid State Chemistry* 180 (2007) 3545.
- [34] S.M. Griffiths, et al., *Analytical Chemistry* 83 (2011) 3778.
- [35] Y. Liu, et al., *Toxicology Letters* 204 (2011) 183.
- [36] W. Wu, et al., *International Journal of Nanomedicine* 5 (2010) 1079.
- [37] R.D. Oude Engberink, et al., *Radiology* 243 (2) (2007) 467.
- [38] J. Kristl, et al., *International Journal of Pharmacy* 256 (2003) 133.